

1 Wavelet Phase Coherence of Ictal Scalp EEG-Extracted
2 Muscle Activity (SMA) as a Biomarker for Sudden
3 Unexpected Death in Epilepsy (SUDEP)

4 Adam C. Gravitis¹, Krishram Sivendiran^{1*}, Uilki Tufa¹, Katherine Zukotynski^{2,3}, Yotin Chinvarun⁴, Orrin
5 Devinsky⁵, Richard Wennberg⁶, Peter L. Carlen^{1,6} and Berj L. Bardakjian^{1,3†}

6 *Co-first author, †Corresponding author

7 ¹ Institute of Biomedical Engineering, University of Toronto, Toronto, ON, Canada

8 ² Department of Radiology, McMaster University, Hamilton, ON, Canada

9 ³ Department of Electrical and Computer Engineering, University of Toronto, Toronto, ON, Canada

10 ⁴ Department of Medicine, Phramongkutklao Royal Army Hospital, Bangkok, Thailand

11 ⁵ Grossman School of Medicine, New York University, New York, NY, United States

12 ⁶ Department of Medicine (Neurology), University of Toronto, Toronto, ON, Canada

13

14

15 **Abstract**

16 *Objective.* Approximately 50 million people worldwide have epilepsy and 8-17% of the deaths in patients with
17 epilepsy are attributed to sudden unexpected death in epilepsy (SUDEP). The goal of the present work was to
18 establish a biomarker for SUDEP so that preventive treatment can be instituted. *Approach.* Seizure activity in
19 patients with SUDEP and non-SUDEP was analyzed, specifically, the scalp EEG extracted muscle activity (SMA)
20 and the average wavelet phase coherence (WPC) during seizures was computed for two frequency ranges (1-12 Hz,
21 13-30 Hz) to identify differences between the two groups. *Main results.* Ictal SMA in SUDEP patients showed a
22 statistically higher average WPC value when compared to non-SUDEP patients for both frequency ranges. Area
23 under curve for a cross-validated logistic classifier was 81%. *Significance.* Average WPC of ictal SMA is a
24 candidate biomarker for early detection of SUDEP.

25

26 **Introduction**

27

28 Epilepsy is a common chronic neurological disorder characterized by recurrent seizures. Sudden unexpected death in
29 epilepsy (SUDEP) occurs in approximately 1 in 1000 people with epilepsy each year [1] and typically occurs after
30 convulsive seizures in sleep, followed by cardio-respiratory dysfunction and impaired arousal which may be caused
31 by spreading depression or epileptiform activity involving the brainstem [1-6]. A biomarker for epilepsy patients at
32 high SUDEP risk could enable earlier and more aggressive preventive interventions. Electromyography (EMG) can
33 detect tonic-clonic seizures [7]. Scalp muscle activity (SMA) has been shown as a useful diagnostic for detection of
34 tonic-clonic seizures, an established risk factor for SUDEP [8-9]. In our retrospective study, since limb EMG was
35 not recorded, we extracted electrical muscle activity from scalp electrodes (i.e., SMA). Ictal SMA had an average
36 wavelet phase coherence (WPC) in two frequency ranges that was significantly different in the SUDEP group as
37 compared to the non-SUDEP group, identifying average WPC as a candidate biomarker for SUDEP.

38

39 **Method**

40 *Data Acquisition*

41 Scalp EEG recordings were obtained from 5 non-SUDEP and 7 definite SUDEP patients (sudden, unexpected death
42 of a patient without relevant comorbidities, in which postmortem examination, including toxicology, does not reveal

43 a cause of death other than epilepsy). Non-SUDEP controls were selected based on their similarity to SUDEP patients.
44 EEG recordings were acquired using the Natus/Xltek EEG system with 19 or more electrodes. Although no recorded
45 seizures were fatal, all SUDEP patients died within 3 years of their last available recordings. Patients categorized as
46 non-SUDEP did not die within 10 years of their last available recordings.

47 Patients were undergoing presurgical evaluation in an epilepsy monitoring unit (EMU), with drug-resistant focal
48 (temporal or extratemporal lobe) epilepsy and were not on anti-seizure medications at the time of recording. Apart
49 from their definite SUDEP designation, the following data were not available in this retrospective study: simultaneous
50 video EEG, sleep/wakefulness states, other medications, MRI findings, or non-epilepsy medical history.

51 The data were obtained through the consortium formed by the Toronto Western Hospital, the New York University
52 (NYU) Comprehensive Epilepsy Center, and the Phramongkutklao Royal Army Hospital (Tables I and II). Ictal
53 durations were identified from EEG scalp electrode recordings by board-certified neurologists/
54 electroencephalographers (Table 1).

Patient	Classification	Age	Sex	Sampling Rate [Hz]	# of Ictal Recordings	Range of Ictal Durations [s]
1	non-SUDEP	28	M	500	2	73 - 126
2	non-SUDEP	19	M	512	3	60 - 138
3	non-SUDEP	42	F	512	1	86
4	non-SUDEP	40	F	512	1	69
5	non-SUDEP	28	M	512	5	54 - 109
6	SUDEP	13	M	256	2	76 - 84
7	SUDEP	21	F	256	1	241
8	SUDEP	43	F	512	6	62 – 272
9*	SUDEP	47	M	200	3	110 – 474
10	SUDEP	30	M	256	1	117
11**	SUDEP	47	F	500	1	63

55
56 **Table 1.** Ictal Patient Data (*one seizure from patient 9 was reserved for risk
57 assessment; ** one interictal segment from patient 11 was reserved for autocorrelation
58 threshold selection, per Table 2).

Patient	Classification	Age	Sex	Sampling Rate [Hz]
11**	SUDEP	47	F	500
12	SUDEP	26	F	512

60 **Table 2.** Interictal Patient Data, used for autocorrelation threshold selection
61

62 *Protocol Approvals and Data Availability*

63 The institutional review boards of the multi-centre consortium approved the study protocols and all patients gave
64 informed consent. The anonymized datasets used in this study are available upon request. They are not publicly
65 available due to institutional restrictions associated with original data acquisition protocols.

66 *SMA Extraction and Analysis*

67 (1) Original EEG recordings ranged in sampling rate from 200 Hz to 512 Hz. All recordings were upsampled to
68 512 Hz, and low-pass filtered at 100 Hz. (2) EEG signals from each of the 19 standard electrodes of the international
69 10-20 system were decomposed into 30 components using singular spectrum analysis (SSA). (3) Notch filtering of 60
70 Hz and its harmonics. (4) Autocorrelation values for each SSA component were calculated. (5) An autocorrelation
71 threshold was tuned to maximize EMG-like properties of extracted signal. (6) SSA components below the tuned
72 autocorrelation threshold were extracted as EMG-like SMA signals. (7) WPC was calculated between retained
73 components of each electrode pair. (8) Average values of WPC over ictal duration and 1-12 Hz and 13-30 Hz ranges
74 were calculated. (9) Per-seizure spatial averages of WPC were derived from per-electrode temporal averages.

75

76 **Figure 1.** Block diagram showing methodology: the shown interictal EEG trace is from patient 12.

77 Retained SSA components below the tuned autocorrelation threshold ($R < 0.8$) were summed to form the
78 extracted SMA signal, which was analyzed in two frequency ranges: 1-12 Hz and 13-30 Hz.

79

80 Reported differences between EEG and EMG signals [10] were reflected in the extracted SMA and retained EEG
81 resulting from this methodology (Fig. 2). Extracted SMA, selected for lower autocorrelation values, had dominant
82 power above 50 Hz, but also included activity in the 1-30 Hz range. Retained EEG was selected for higher
83 autocorrelation and resulting in dominant power below 50 Hz.

84

85 **Figure 2.** WPC of extracted SMA and retained EEG against raw electrode for patient 12.

86

87 *Singular Spectrum Analysis (SSA)*

88 SSA using elementary grouping [10] was first performed on raw EEG data from ictal recordings to decompose the
89 signal into its constituent components. This technique consists of first creating a trajectory matrix, T , from lagged
90 versions of the time series x (in this case, a single EEG electrode recording). Next, the singular value decomposition
91 of the trajectory matrix was taken. Using values obtained from this decomposition, the trajectory matrix was
92 decomposed into a sum of L elementary matrices (matrices that have a rank of 1), where U and V were obtained from
93 the singular value decomposition of the trajectory matrix, λ represents the eigenvalues of the trajectory matrix and k
94 ranges from 0 to $L-1$.

95

96
$$T = \sum_k \sqrt{\lambda_k} U_k V_k^T \quad (1)$$

97

98 Finally, each of the L elementary matrices were hankelized and each resulting Hankel matrix was converted into a
99 time series, where each diagonal value of the Hankel matrix corresponds to a sample in the time series.

100 *Autocorrelation Analysis*

101 The autocorrelation of each SSA component was computed following equation (2) [10], where E is the expected
102 value operation, $s_1(t)$ is the SSA component time series and $s_2(t) = s_1(t-1)$.

103

104
$$R = \frac{E[(s_1(t) - E(s_1(t)))(s_2(t) - E(s_2(t)))]}{\sqrt{E[(s_1(t) - E(s_1(t)))^2]E[(s_2(t) - E(s_2(t)))^2]}} \quad (2)$$

105

106 As muscle activity has a wide frequency range, it has a lower autocorrelation value than EEG signals. Reference
107 [10] demonstrated an autocorrelation threshold can be used to differentiate an EEG signal from scalp muscle activity.
108 We apply the technique to extract SMA from EEG.

109 The SSA components identified as EEG were removed and the remaining components summed to recover SMA.

110 *Autocorrelation Threshold Selection*

111 Our analysis depended on an autocorrelation threshold value to distinguish extracted muscle activity from EEG
112 rhythms (Fig. 3(b)). Autocorrelation thresholds between 0.5 and 0.95 were tested, at 0.05 intervals. Five inter-ictal

113 EEG segments of SUDEP patients were used as controls, each spanning 62 s, and were processed to obtain resulting
114 SMA signals for each threshold value. All control recordings were obtained from 2 SUDEP patients (2 from patient
115 11, 3 from patient 12) and were used for threshold tuning (Table 2).

116

117 **Figure 3.** Autocorrelation threshold tuning. (A) Power spectra of extracted and retained signals for
118 varying autocorrelation thresholds. (B) Comparison of average WPC between extracted SMA and raw
119 electrode for 1-30 Hz and 30-100 Hz ranges: 0.75-0.85 maximized this difference. (C) The log of the ratio
120 of extracted power between 50-70 Hz at different autocorrelation thresholds.

121

122 The WPC between each of the 5 resulting SMA signals and their corresponding scalp electrodes at each
123 autocorrelation threshold. Electrodes FZ, FP1 and FP2 were selected due to the high presence of scalp muscle activity
124 when compared to other electrodes, due to proximity of facial muscles. Each data matrix was averaged over time and
125 averaged over two frequency ranges: 1-30 Hz and 31-100 Hz.

126 Fig. 3(b) shows the change in average WPC between extracted SMA and raw electrode for both 1-30 Hz and 31-
127 100 Hz frequency ranges for varying autocorrelation thresholds. A threshold of 0.8 was selected as it maximized the
128 difference between EMG-like retained SMA and retained EEG, based on power spectra (Fig. 3(a)), WPC (Fig. 3(b)),
129 and ratio of power in the 50-70 Hz range (Fig. 3(c)).

130 Phase-phase cross-frequency coupling (PPC) analysis was performed between the extracted SMA and
131 corresponding electrode for an ictal segment from patient 11 (Fig. 2), using an $n:m$ PPC calculation [11-12]:

132

$$133 \quad PPC = \left| \frac{1}{T} \sum_{t=1}^T e^{i(n\theta_1(t) - m\theta_2(t))} \right|$$

134

135 PPC analysis (Fig. 4(b)) confirmed strong coupling between the 50-70 Hz EMG-like frequencies of the raw
136 electrode with lower frequencies of extracted SMA, most pronounced at 12-15 Hz.

137

138

139 **Figure 4.** Phase coupling of extracted SMA with EMG signal in ictal segment of patient 12. (A) Raw ictal
140 EEG, Extracted SMA, and Retained EEG. (B) Phase-phase cross-frequency coupling (PPC) between
141 extracted SMA and raw electrode (left), and between retained EEG and raw electrode (right). Lower
142 frequencies of extracted SMA are strongly coupled with higher frequencies of EMG.

143

144 *Wavelet Phase Coherence*

145 The WPC of the SMA signals were obtained for each electrode pair. Since 19 electrodes from each ictal recording
146 were used in the analysis, this resulted in 361 (19 x 19) WPC data matrices. For each data matrix, a time average was
147 performed over the entire duration of the seizure. A frequency average was then performed over 1-12 Hz and 13-30
148 Hz.

149 Disregarding coherence entries between identical electrodes, each row of the resulting matrix was then averaged
150 over the 18 column entries to obtain the average WPC on a per-electrode basis. To obtain the average WPC on a per
151 seizure basis, each group of 19 electrodes was averaged.

152 *Estimation Statistics*

153 Results are presented using estimation statistics as an alternative to null hypothesis significance testing [13].

154 *Risk Assessment*

155 A logistic classifier was trained on the WPC values of both frequency bands of interest to produce a propensity
156 score. One seizure from Patient 9 was withheld from training, in order to validate the risk assessment produced by
157 the classifier.

158

159 **Results**

160 *Validation of SMA Extraction*

161 We hypothesized that the WPC of retained (following SMA removal) EEG would be distinct from that of the
162 extracted SMA, as an initial validation of the extraction process.

163 Using the optimal autocorrelation threshold of 0.8, SMA was extracted from 5 SUDEP (12 seizure recordings) and
164 5 non-SUDEP (12 seizure recordings) patients. However, instead of discarding the SSA components which
165 corresponded to an autocorrelation value greater than or equal to 0.8, the components were summed to obtain the

166 retained EEG signal.

167 Next, average WPC was computed on a per electrode basis for the SMA and retained EEG signals. For both
168 frequency ranges: 1-12 Hz and 13-30 Hz, Fig. 5(a) compares the average WPC for both signals for SUDEP patients
169 and Fig. 5(b) compares the average WPC for both signals for non-SUDEP patients.

170

171

172 **Figure 5.** Comparing the average wavelet phase coherence (WPC) of scalp EEG-extracted muscle
173 activity (SMA) and retained (following SMA removal) EEG networks from entire ictal recordings on a per
174 electrode basis (19 electrodes used per recording) for two frequency ranges: 1-12 Hz and 13-30 Hz. (A)
175 For 5 SUDEP patients. (B) For 5 non-SUDEP patients.

176

177 *Comparing Average WPC*

178 The average WPC was computed on a per-electrode and per-seizure basis for each of the 13 SUDEP seizures and
179 each of the 12 non-SUDEP seizures. Comparing non-SUDEP to SUDEP patients, the average WPC was significantly
180 higher for SUDEP patients for each of the frequency ranges, as shown in Fig. 6 and 7.

181

182

183

184 **Figure 6.** (A) Comparing the average wavelet phase coherence (WPC) over 1-12 Hz for scalp EEG-
185 extracted muscle activity (SMA) networks from entire ictal recordings for 5 SUDEP patients (12 seizures)
186 and 5 non-SUDEP patients (12 seizures) on a per electrode basis (19 electrodes used per recording), left,
187 and mean of all electrodes per seizure, right. (B) Controlling for GTC seizures only, comparing the
188 average WPC over 1-12 Hz for SMA networks from entire ictal recordings for 4 SUDEP patients (9 GTCS)
189 and 4 non-SUDEP patients (8 GTCS).

190

191

192

193 **Figure 7.** (A) Comparing the average WPC over 13-30 Hz for SMA networks from entire ictal recordings
194 for 5 SUDEP patients (12 seizures) and 5 non-SUDEP patients (12 seizures) on a per electrode basis (19
195 electrodes used per recording), left, and mean of all electrodes per seizure, right. (B) Controlling for GTC
196 seizures only, comparing the average WPC over 13-30 Hz for SMA networks from entire ictal recordings
197 for 4 SUDEP patients (9 GTCS) and 4 non-SUDEP patients (8 GTCS).

198

199 *Risk Assessment*

200 The logistic classifier resulted in a Receiver Operating Characteristic (ROC) curve with an Area Under Curve
201 (AUC) of 97% for training data. The SUDEP seizure withheld for testing was correctly classified as SUDEP by this
202 method.

203

204

205 **Figure 8.** Logistic classifier trained on 1-12 Hz and 13-30 Hz WPC values. (A) ROC curve of training
206 data: Accuracy optimized point (red), used to determine classifier decision threshold. (B) Mean seizure
207 propensity scores, with standard error shown. (C) Propensity score of seizure not included in training set
208 from SUDEP patient. (D) ROC curve for leave-one-out cross-validation, over 10 rounds.

209

210 **Discussion**

211 We found that average WPC was significantly higher for SUDEP compared to non-SUDEP patients for both
212 frequency ranges. Average WPC of SMA is a measure of scalp muscle coherence, as strong contractions would be
213 captured by more electrodes and result in a higher average WPC value. This is in line with previous studies using
214 EMG-EMG coherence in myoclonus assessment in epileptic patients. The possibility that stronger contractions
215 observed in SUDEP patients were due only to the propensity of SUDEP patients to have generalized tonic-clonic
216 seizures [9] was negated as significant differences held in both bands when comparing GTCS only. Further, the risk
217 assessment based on logistic classification of resulting WPC values demonstrated the clinical application of these
218 measures.

219 This study compared WPC of EMG-like SMA from ictal EEG recordings, as EMG recordings of SUDEP patients
220 were not available. Epilepsy patients treated in an EMU are typically recorded for EEG and ECG; less often for EMG.
221 High-quality ictal EMU recordings of SUDEP patients remain rare; EMG recordings are rarely available for study.
222 Our technique establishes a pathway to using SMA extracted from ictal scalp EEG recordings to leverage EMG-related
223 biomarkers of SUDEP.

224 This work expands on previous studies [14] extracting EMG-like SMA from EEG recordings. When extracting
225 SMA, there was minimal loss in scalp muscle activity and minimal contamination of EEG signal and noise during the
226 extraction to ensure SMA signals were not distorted or contaminated. SSA was selected as its decomposition process
227 was able to separate the scalp muscle activity signal components from the EEG signal components, in contrast to
228 similar algorithms which were investigated such as ensemble empirical mode decomposition.

229 Differences in muscular contractions may result from brainstem network disruption implicated in SUDEP.
230 Hypothetical models in rats have suggested that convulsions can result directly from self-sustained epileptic activation
231 in brainstem structures [15], and that these convulsions differ from those originating from the motor cortex. The
232 significantly stronger WPC between extracted SMA in this study may be attributable to convulsions driven by the
233 reticular core of near-SUDEP brainstems.

234 EMG analysis can detect tonic-clonic seizures in isolation [7, 9] and in multimodal sensory environments [16-17].
235 Several methods for classification of EMG features have been reported. Empirical mode decomposition of EMG has
236 been used to classify upper limb movements [18], while techniques based on discrete wavelet transforms of EMG
237 have identified muscle movements [19-21].

238 Video-EEG remains the clinical gold standard for identifying seizures leading to a scarcity of EMG recordings in
239 SUDEP patients. Therefore, it is important to extract EMG features from other modalities. Using only EEG recordings,
240 [22] applied principal component analysis, and both linear discriminant analysis and support vector machines to
241 identify jaw movement, without explicitly identifying EMG. Reference [23] developed an automated system to
242 identify seizures based on ‘optical flow’ of recorded motion. In this study, EMG features were extracted from scalp
243 EEG using SSA.

244 An EMG-based SUDEP biomarker has been proposed, observing that EMG-derived respiration features identified
245 ictal laryngospasms in mouse models [14]. This possibility was reinforced by a case report of a near-SUDEP patient
246 consistent with this pattern [24].

247 Investigations of high frequency oscillations (HFOs) in EEG of patients with epilepsy revealed that they were
248 typically of low amplitude and a phase-based measure such as WPC was required for their analysis. Previous work
249 from our team demonstrated that WPC applied to intracranial EEG recordings helped characterize HFOs (80-400 Hz),
250 across brain sites in patients with extratemporal lobe epilepsy that localized seizure onset sites [25]. Subsequent work
251 by the same authors suggested strong coherence between HFO sites in the ictal state, and also in low frequency
252 oscillations (LFOs), 5-12 Hz sites in the interictal state, can localize the same seizure onset sites [26]. Our team also
253 previously reported differences in EEG WPC during infantile epileptic spasms [27].

254

255 **Conclusion**

256 SSA with an autocorrelation threshold was an effective method of extracting SMA when using the novel threshold
257 tuning technique mentioned in this paper. The results show that average WPC of ictal SMA is a biomarker for SUDEP.
258 Future research should consider using additional seizure data containing corresponding EMG recordings to help
259 establish a more robust threshold for differentiating scalp muscle activity from brain activity and evaluating additional
260 SUDEP and non-SUDEP ictal SMA data.

261

262 **Acknowledgements**

263 B.L. Bardakjian would like to acknowledge support by the Epilepsy Research Program (EpLink) of the Ontario
264 Brain Institute (OBI), the Natural Sciences and Engineering Research Council of Canada (NSERC), and the SciNet
265 HPC Consortium funded by the Canada Foundation for Innovation; the Government of Ontario; Ontario Research
266 Fund (Research Excellence); and the University of Toronto.

267

268 **References**

269

- 270 [1] O. Devinsky, "Sudden, unexpected death in epilepsy," *N. Engl. J. Med.* 2011;365(19):1801-11. doi:10.1056/NEJMra1010481.
- 271 [2] J.G.R. Jefferys *et al*, "Brainstem activity, apnea, and death during seizures induced by intrahippocampal kainic acid in anaesthetized rats," *Epilepsia*. 2019;60:2346-58. doi:10.1111/epi.16374.
- 272 [3] A. Murugesan *et al*, "Postictal serotonin levels are associated with peri-ictal apnea," *Neurology*. 2019;93:1485-94.
273 doi:10.1212/WNL.0000000000008244.
- 274 [4] S. Patodia *et al*, "The ventrolateral medulla and medullary raphe in sudden unexpected death in epilepsy," *Brain*. 2018;141:1719-33.
275 doi:10.1093/brain/awy078.

277 [5] L. Vilella *et al*, “Postconvulsive central apnea as a biomarker for sudden unexpected death in epilepsy (SUDEP),” *Neurology*. 2019;92:171–
278 182. doi:10.1212/WNL.0000000000006785.

279 [6] Q. Zhan *et al*, “Impaired Serotonergic Brainstem Function during and after Seizures,” *J. Neurosci.* 2016;36: 2711–22.
280 doi:10.1523/jneurosci.4331-15.2016.

281 [7] C. Szabó *et al*, “Electromyography-based seizure detector: preliminary results comparing a generalized tonic-clonic seizure detection
282 algorithm to video-EEG recordings,” *Epilepsia*. 2015;56(9):1432–37.

283 [8] L. Nilsson *et al*, “Risk factors for sudden unexpected death in epilepsy: a case–control study,” *Lancet*. 1999;353:888–93.

284 [9] S. Beniczky, I. Conradsen, P. Wolf, “Detection of convulsive seizures using surface electromyography,” *Epilepsia*. 2018;59(1):23–29.
285 doi:10.1111/epi.14048.

286 [10] Q. Liu *et al*, “Removal of EMG Artifacts from Multichannel EEG Signals Using Combined Singular Spectrum Analysis and Canonical
287 Correlation Analysis,” *J. Healthc. Eng.* 2019:4159676. doi:10.1155/2019/4159676.

288 [11] P. Tass *et al*, “Detection of n : m Phase Locking from Noisy Data: Application to Magnetoencephalography,” *Phys Rev Lett.* 1998;81(15):
289 3291–4.

290 [12] Gravitis *et al*, “Ictal ECG-based assessment of sudden unexpected death in epilepsy,” *Front. Neurol.* 2023;14:1147576.
291 doi:10.3389/fnur.2023.1147576

292 [13] J. Ho *et al*, “Moving beyond P values: Everyday data analysis with estimation plots,” *Nat Methods*. 2019;16:565–6. doi:10.1038/s41592-019-
293 0470-3

294 [14] M. Stewart *et al*, “Obstructive apnea due to laryngospasm links ictal to postictal events in SUDEP cases and offers practical biomarkers for
295 review of past cases and prevention of new ones,” *Epilepsia*. 2017;58(6):87–90.

296 [15] W. M. Burnham, “Core mechanisms in generalized convulsions,” *Fed Proc.* 1985;44(8):2442–5.

297 [16] A. Van de Vel *et al*, “Non-EEG seizure detection systems and potential SUDEP prevention: State of the art: Review and update,” *Seizure*.
298 2016;41:141–53.

299 [17] F. Leijten, “Multimodal seizure detection: A review,” *Epilepsia*. 2018; 59(1): 42–47.

300 [18] M. Karuna and S. R. Guntur, “EMG Signal Analysis Using Intrinsic Mode Functions to Discriminate Upper Limb Movements,” 2020
301 *International Conference on Artificial Intelligence and Signal Processing (AISP)*, 2020:1–3. doi: 10.1109/AISP48273.2020.9073313.

302 [19] T. Tuncer, S. Dogan, and A. Subasi, “Surface EMG signal classification using ternary pattern and discrete wavelet transform based feature
303 extraction for hand movement recognition,” *Biomedical Signal Processing and Control*, 2020;58:101872.

304 [20] M. Arozi *et al*, “Electromyography (EMG) signal recognition using combined discrete wavelet transform based on Artificial Neural Network
305 (ANN),” 2016 *2nd International Conference of Industrial, Mechanical, Electrical, and Chemical Engineering (ICIMECE)*, 2016: 95–99.
306 doi:10.1109/ICIMECE.2016.7910421.

307 [21] F. Duan *et al*, “sEMG-Based Identification of Hand Motion Commands Using Wavelet Neural Network Combined With Discrete Wavelet
308 Transform,” *IEEE Transactions on Industrial Electronics*. 2016; 63(3):1923–34. doi:10.1109/TIE.2015.2497212.

309 [22] M. S. Bascil, “A New Approach on HCI Extracting Conscious Jaw Movements Based on EEG Signals Using Machine Learnings,” *J Med
310 Syst.* 2018; 42(169). doi:10.1007/s10916-018-1027-1

311 [23] E. Geertsema *et al*, “Automated video-based detection of nocturnal convulsive seiuzures in a residential care setting,” *Epilepsia*. 2018;
312 59(1):53-60.

313 [24] N. Lacuey, L. Vilella, J. Sahadevan, and S. Lhatoo, “Ictal laryngospasm monitored by video-EEG and polygraphy: a potential SUDEP
314 mechanism,” *Epileptic Disorders*. 2018;20(2):146-50.

315 [25] M. Cotic *et al*, “Mapping the coherence of ictal high frequency oscillations in human extratemporal lobe epilepsy,” *Epilepsia*. 2015; 56(3):
316 393-402.

317 [26] M. Cotic *et al*, “Spatial Coherence Profiles of Ictal High-Frequency Oscillations Correspond to Those of Interictal Low-Frequency
318 Oscillations in the ECoG of Epileptic Patients,” *IEEE Transactions on Biomedical Engineering*. 2016;63(1):76-85.
319 doi:10.1109/TBME.2014.2386791.

320 [27] I. Samfira *et al*, “EEG-based spatiotemporal dynamics of fast ripple networks and hubs in infantile epileptic spasms,” *Epilepsia Open*. 2023.
321 doi:10.1002/epi4.1283.

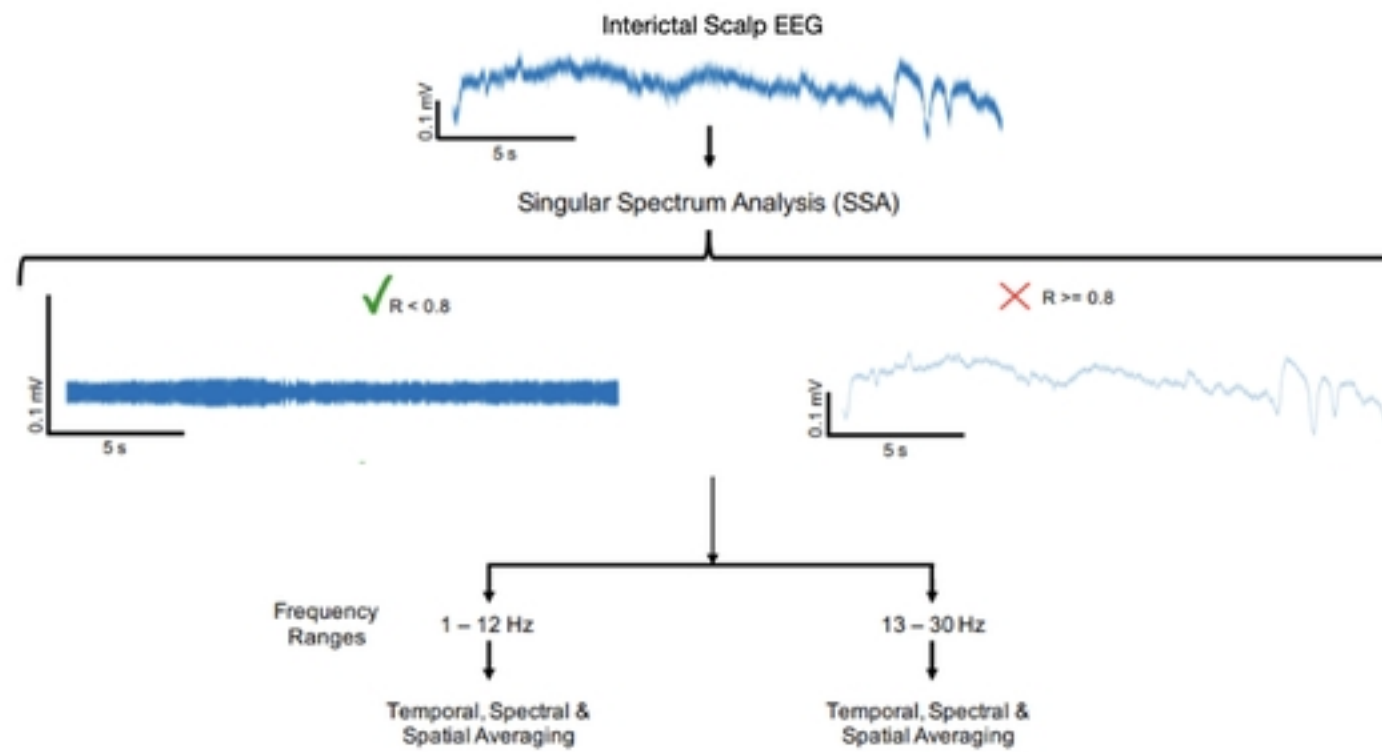


Figure1

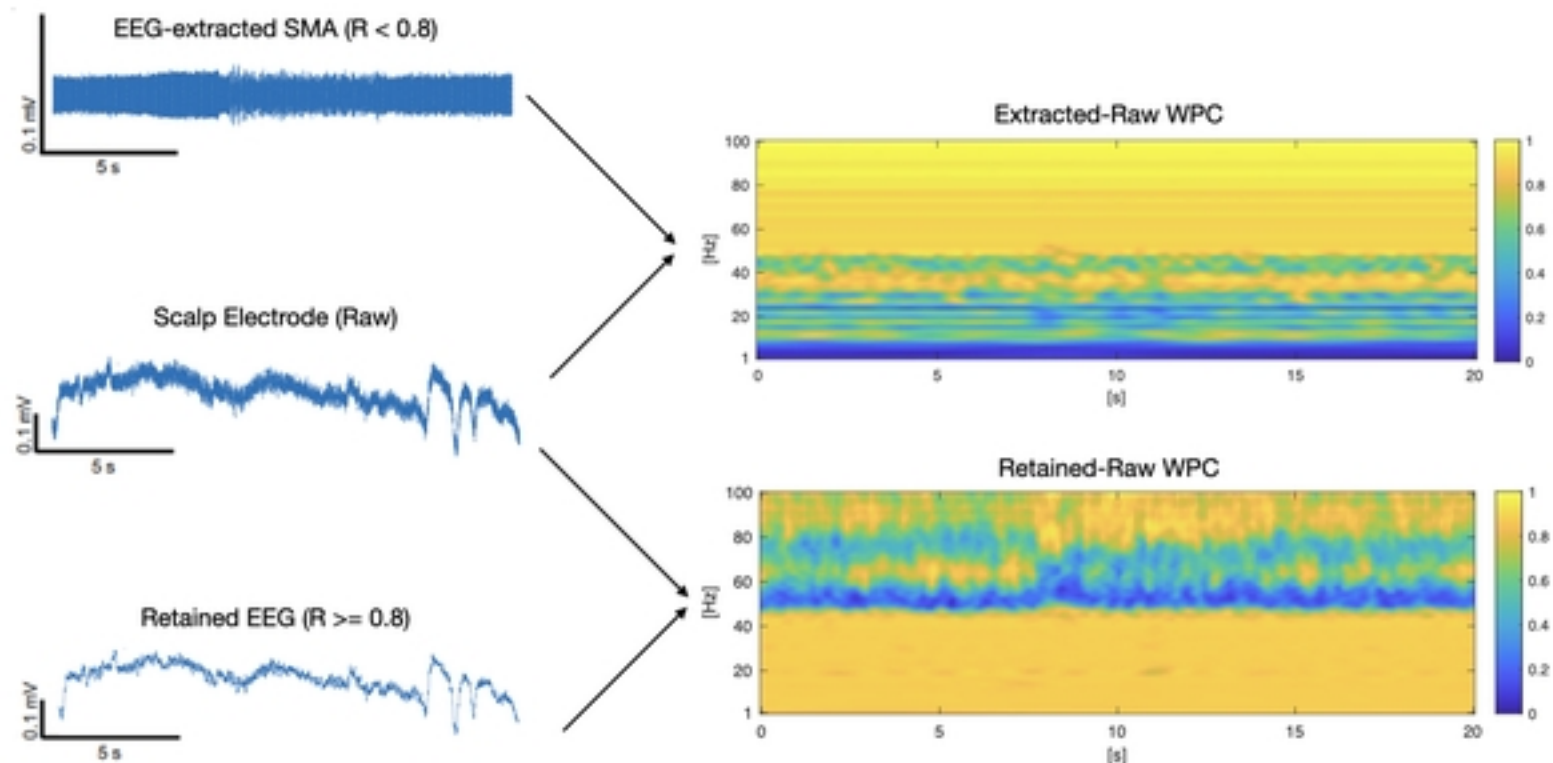
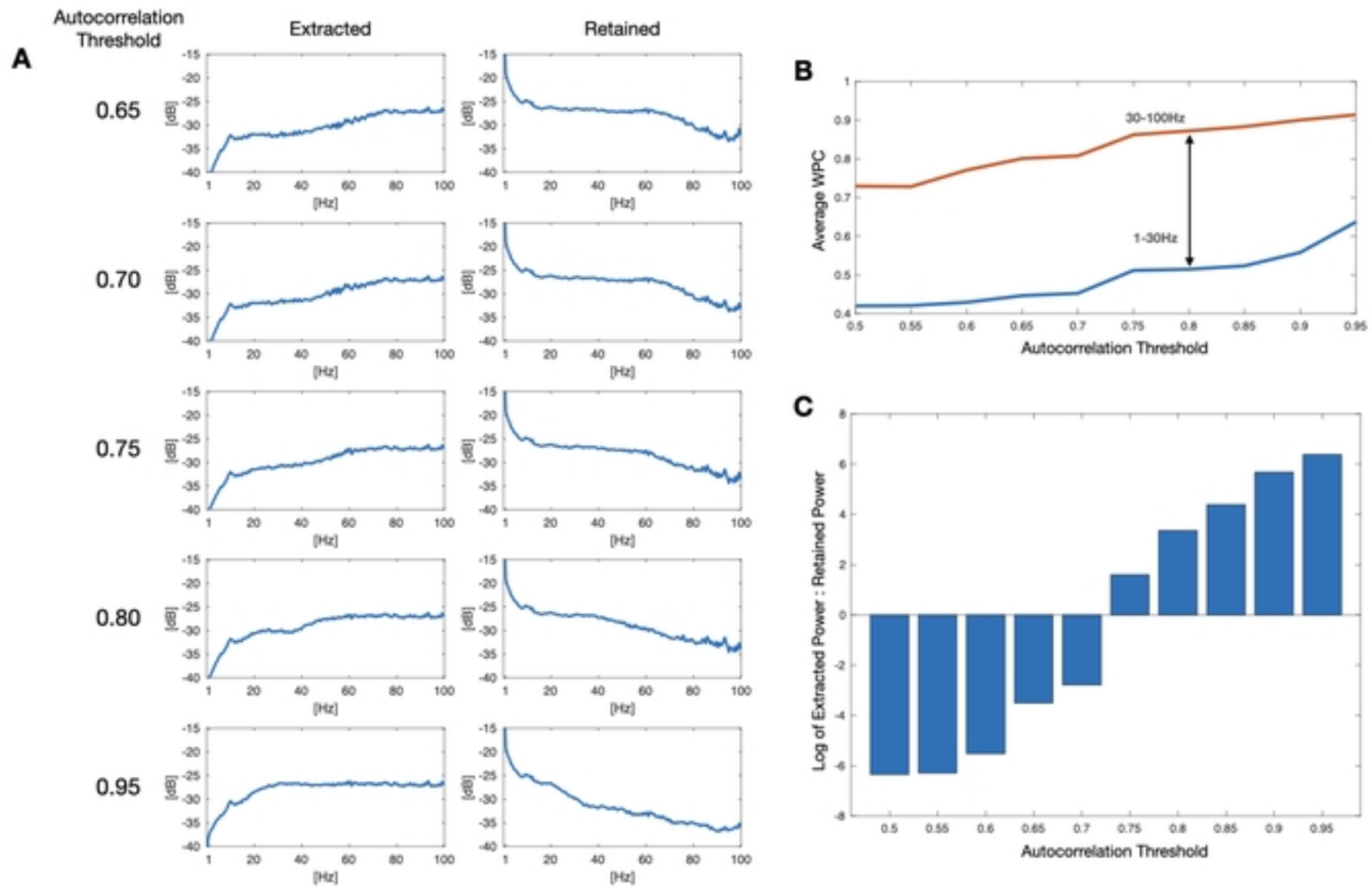


Figure2

Figure3



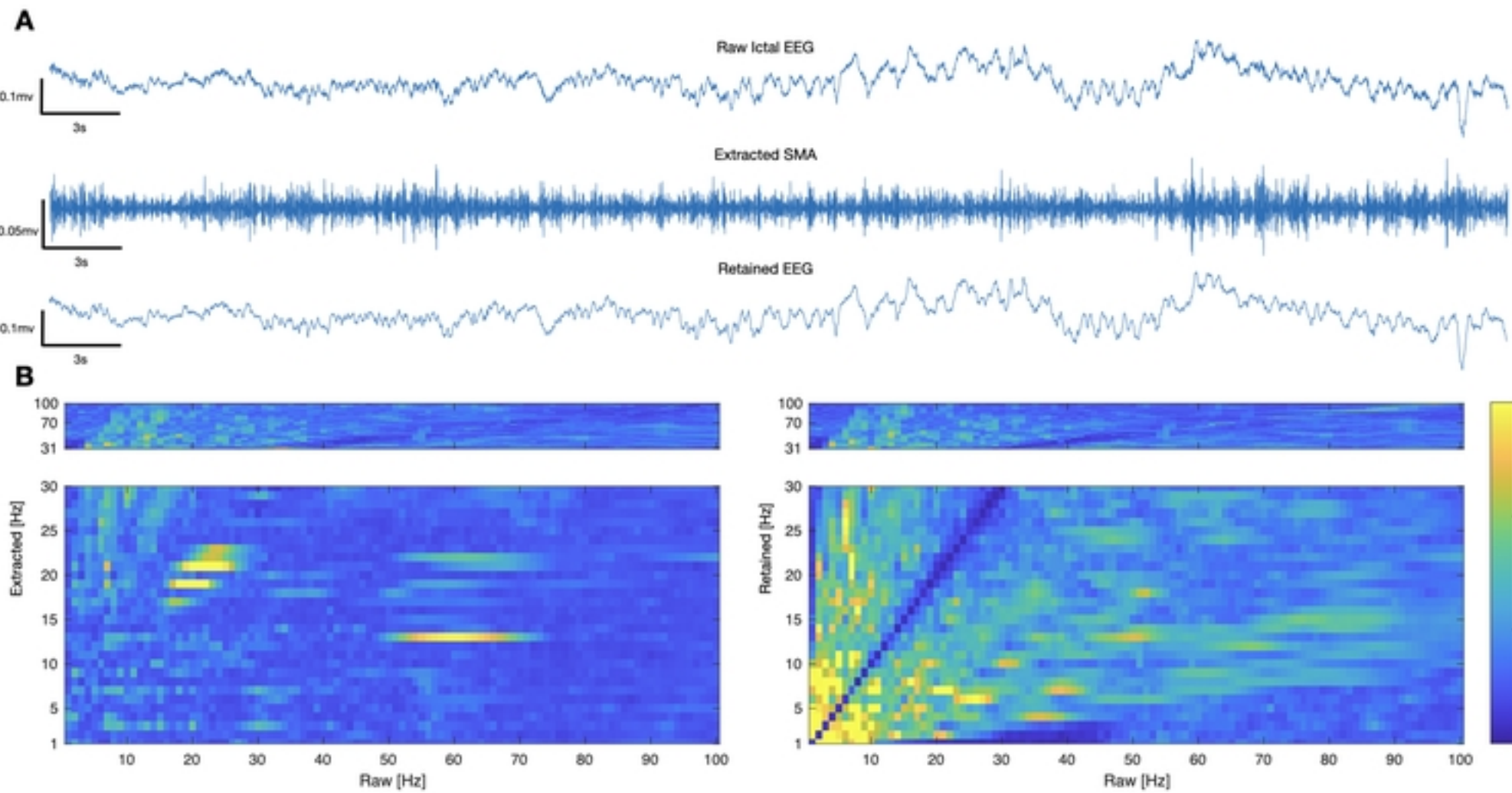
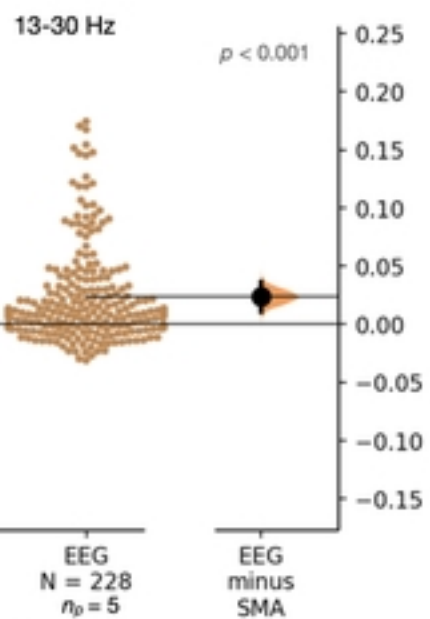
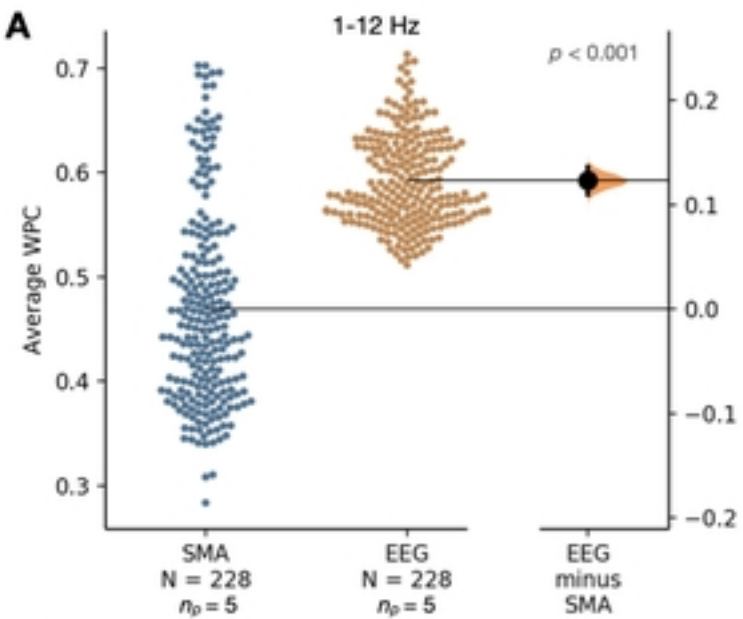
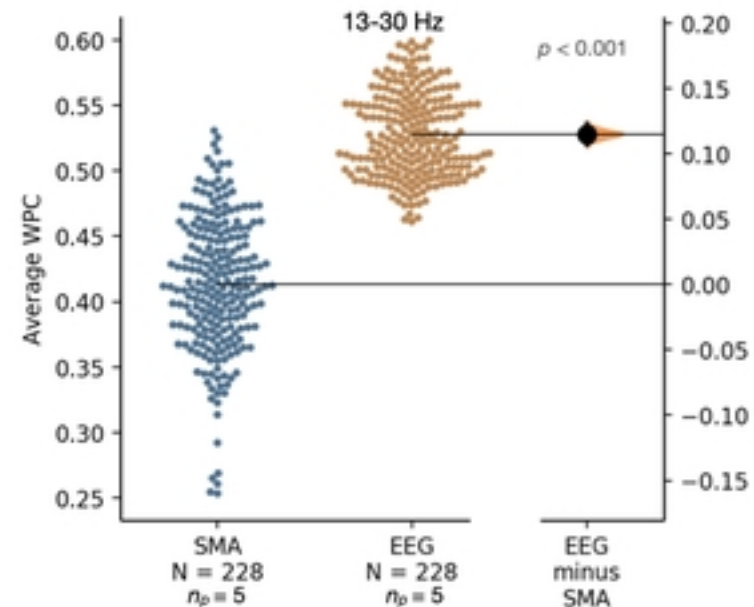
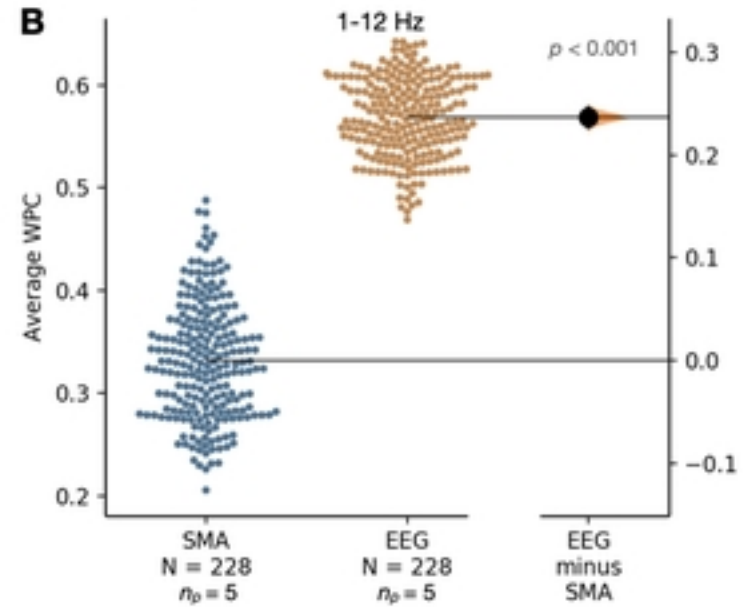


Figure4

A**B****Figure5**

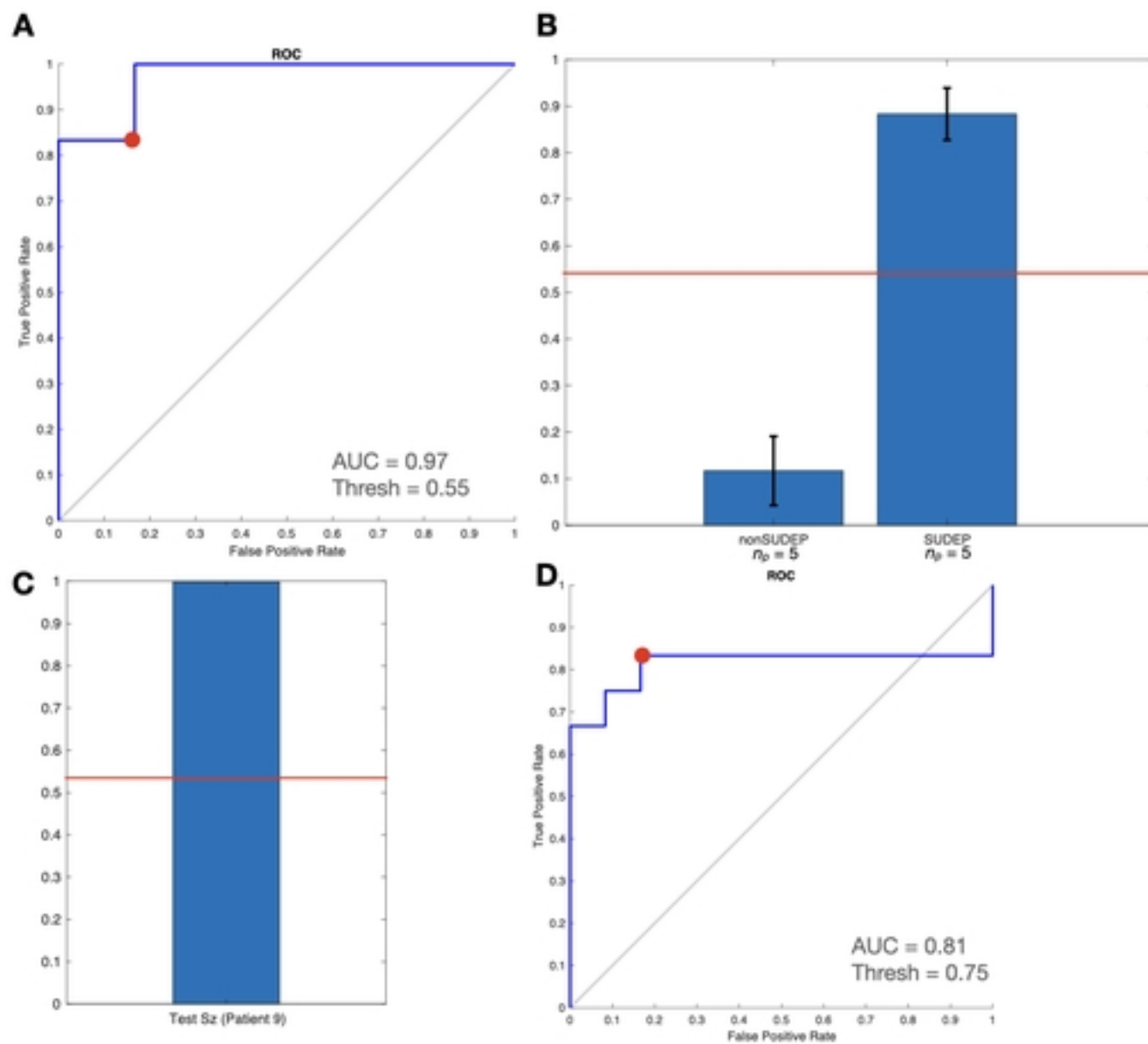
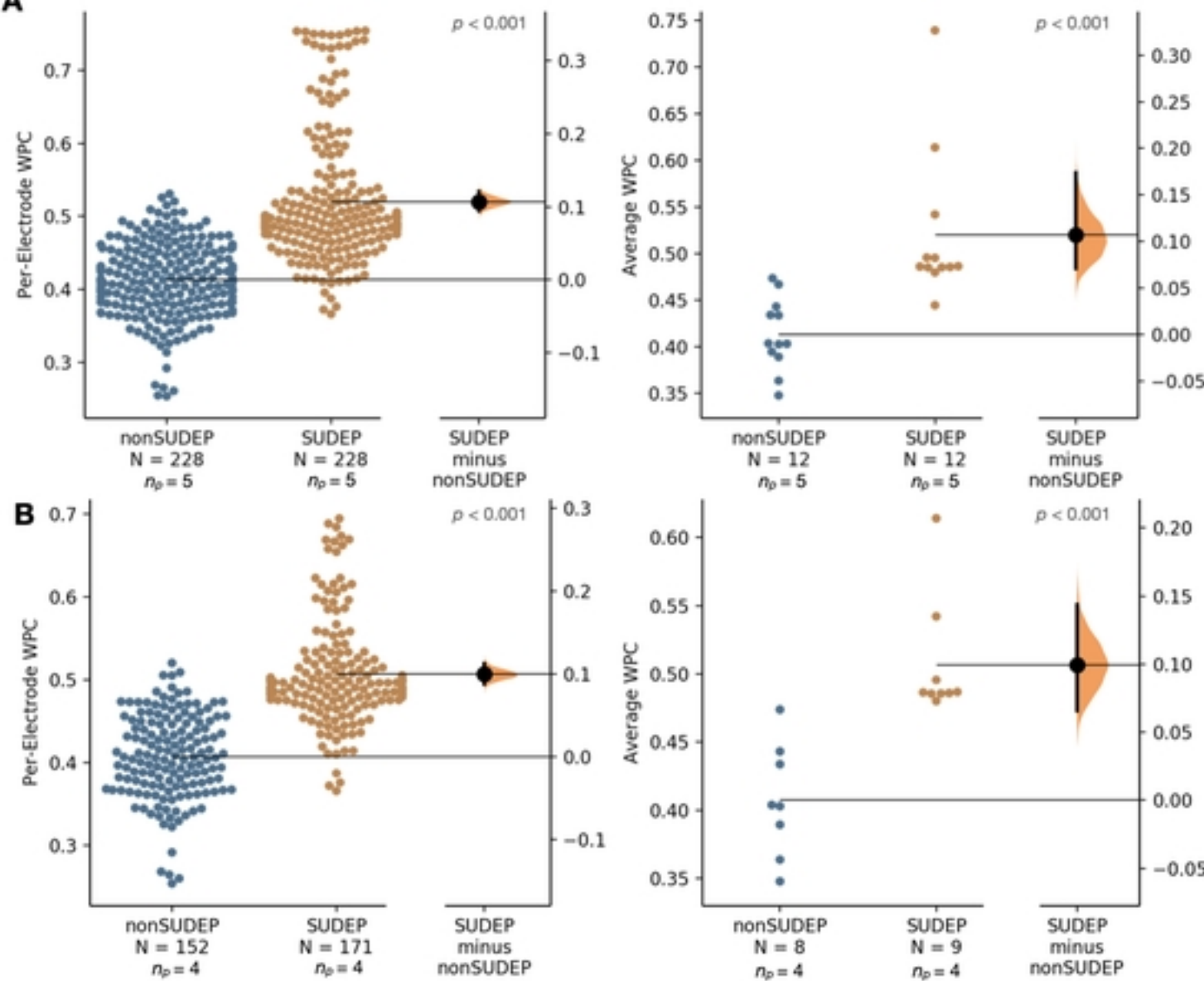
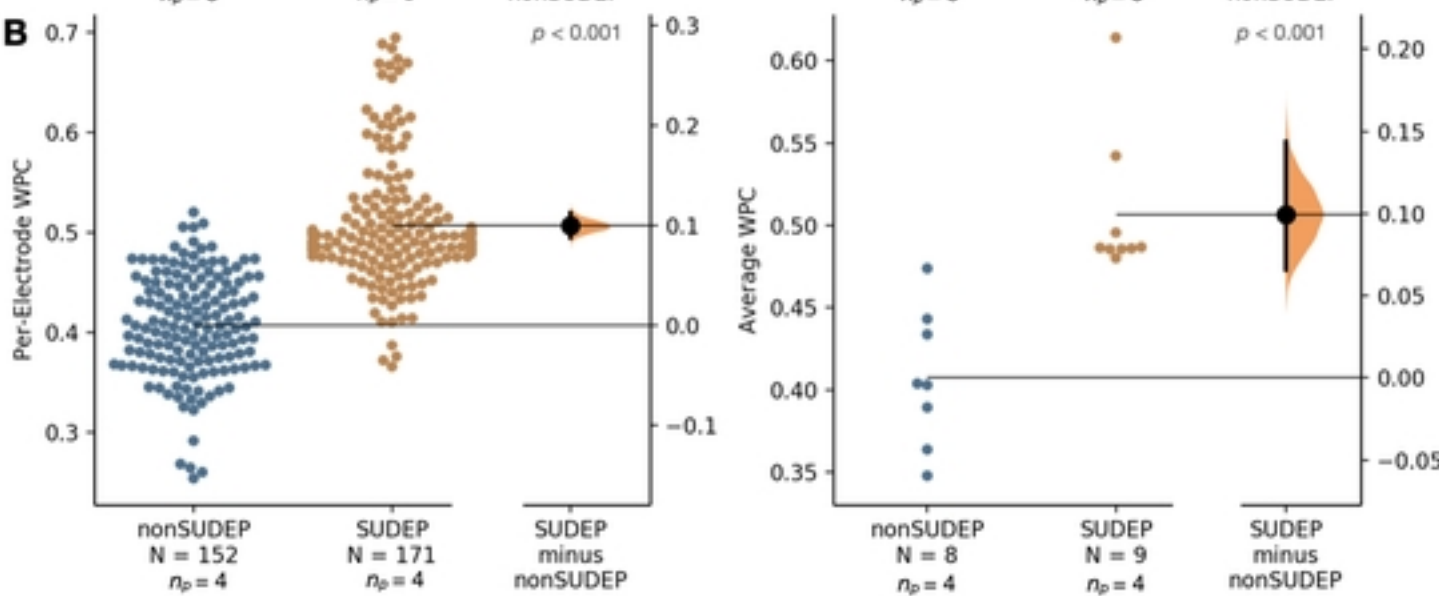
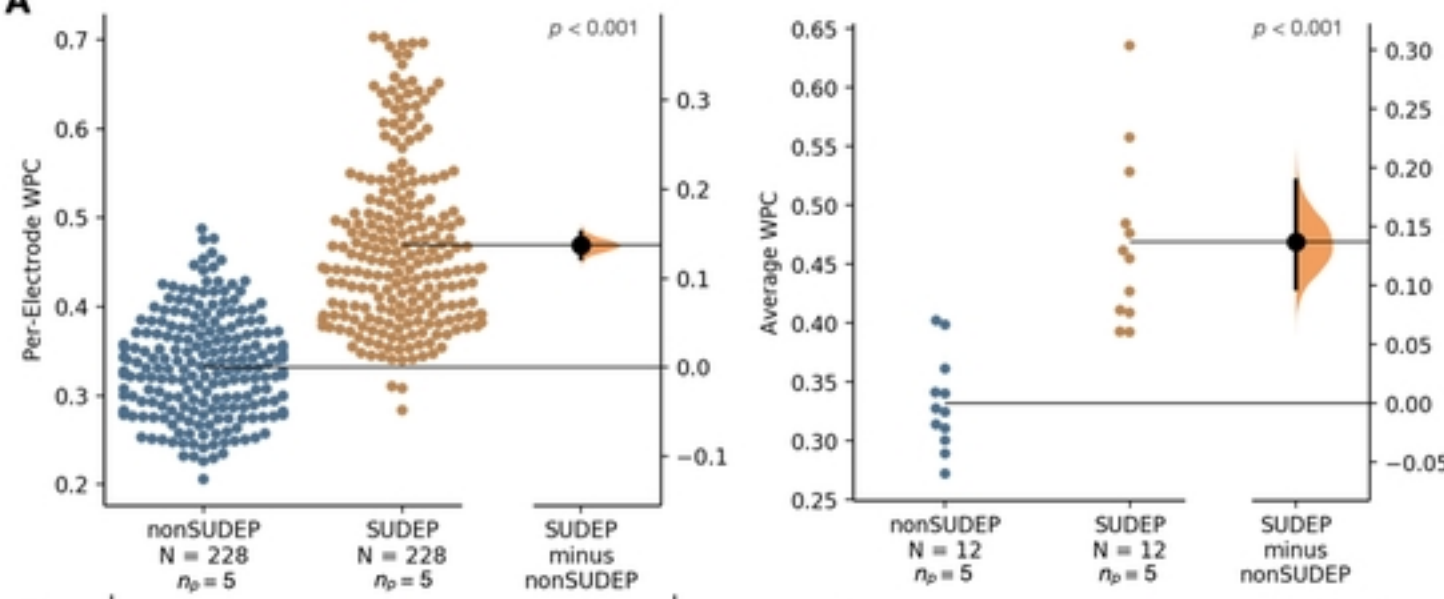
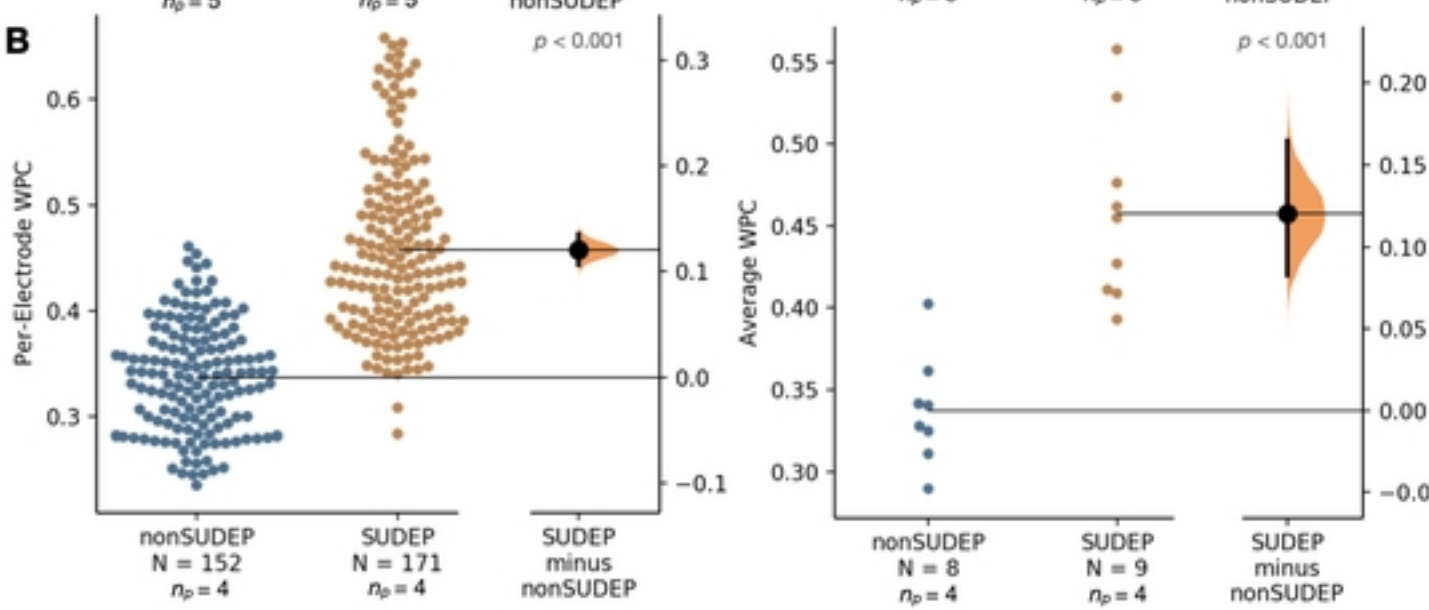


Figure8

A**B****Figure 7**

A**B****Figure 6**